

Piotr Smarzewski

Lublin University of Technology, Faculty of Civil Engineering and Architecture, ul. Nadbystrzycka 40, 20-618 Lublin, Poland
Corresponding author. E-mail: p.smarzewski@pollub.pl

Received (Otrzymano) 06.11.2012

CRACKING ANALYSIS OF REINFORCED CONCRETE BEAM ACCORDING TO PROPOSED METHODOLOGY OF PARAMETER SELECTION OF HIGH STRENGTH CONCRETE

The article presents the analysis of failure for a reinforced concrete beam with a low level of reinforcement, made of high strength concrete, in the process of static deformation in comparison to experimental results. On the basis of its ultimate uniaxial compressive strength, the methodology for defining the parameters of the constitutive model for high strength concrete was developed. The comparison of the obtained results indicates the correctness of the assumptions and constitutive models of the high strength concrete and reinforcement steel, and also the effectiveness of Crisfield's arc length method and the Newton-Raphson iterative solution with adaptive descent. The numerical results of the smeared crack patterns proved to be qualitatively agreeable, regarding the localisation, direction and concentration, with the experimental results.

Keywords: finite element method, reinforced concrete, beam, high strength concrete

ANALIZA STANU ZARYSOWANIA BELKI ŻELBETOWEJ WEDŁUG PROPONOWANEJ METODYKI DOBORU PARAMETRÓW BETONU WYSOKIEJ WYTRZYMAŁOŚCI

W artykule przedstawiono analizę stanu zarysowania belki żelbetowej o niskim stopniu zbrojenia wykonanej z betonu wysokiej wytrzymałości w procesie statycznego odkształcania w porównaniu z wynikami eksperymentalnymi. Zaproponowano metodykę ustalania parametrów modelu konstytutywnego betonu wysokiej wytrzymałości na podstawie jego wytrzymałości na ściskanie. Porównania uzyskanych wyników wskazują na poprawność przyjętych założeń odnośnie do modeli betonu wysokiej wytrzymałości i stali zbrojeniowej, a także na skuteczność metody długości łuku Crisfielda i iteracyjnego rozwiązania Newtona-Raphsona z dostosowanym spadkiem. Wyniki numeryczne wzorów rys rozmytych wykazały jakościową zgodność, co do lokalizacji, kierunku i koncentracji, z wynikami doświadczalnymi.

Słowa kluczowe: metoda elementów skończonych, żelbet, belka, beton wysokiej wytrzymałości

INTRODUCTION

High strength concretes are new construction materials that are increasingly common in the construction industry. The material is characterised by its high strength, low absorbability, low water permeability and high freeze resistance, which results in high durability. They are used in high buildings, drilling platforms, bridges, underground and hydro-technical constructions. Its common use is hindered by a lack of normative regulations and recommendations for design calculations. Admittedly, an increasingly higher number of implementations of new materials in the world construction industry is based on engineers' experience and previous experiments to a larger extent, rather than on theoretical analyses. This results mainly from the high complexity of these composites and the properties that distinguish them from conventional concrete.

Precise simulation of these composites' behaviour under static load requires the consideration of physical

non-linearities of the construction component materials: high strength concrete and reinforcing steel, particularly material softening (non-static material behaviour), interaction on the contact surface between the concrete and steel, and considering the local concentration of large deformations influencing concrete cracking and crushing. In order to solve such a complicated numerical task, it is necessary to construct a spatial model with high density meshing, to consider spatial tensile stresses and deformations, and to use an appropriate method of solving simultaneous equations.

METHODOLOGY OF SELECTING CONCRETE MODEL PARAMETERS

The article presents the analyses of behaviour of a model reinforced high strength concrete beam in the

process of static deformation. The Finite Element Method calculations were performed using the ANSYS program. The numeric model of a spatial reinforced high strength concrete beam uses the dimensions of a simply supported rectangular BP-1a beam, analysed and described by Kamińska in her work [1] - Figure 1.

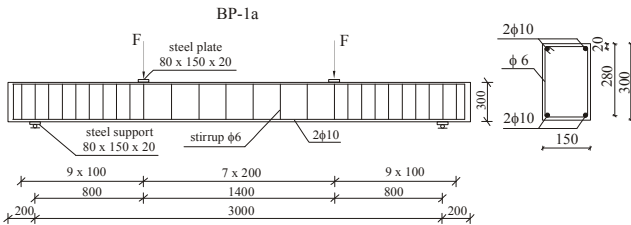


Fig. 1. Dimensions and cross-section of BP-1 beams with reinforcement and loading arrangements

Rys. 1. Wymiary i przekrój poprzeczny belki BP-1a wraz z układem zbrojenia i schematem obciążenia

Considering the longitudinal symmetry of the element, the subject of modelling was $\frac{1}{2}$ of the beam, 1700 mm long, 150 mm wide and 300 mm high. Figure 2 presents a cross-section of the BP-1a beam into finite elements with observation points of variations of deflection and strain.

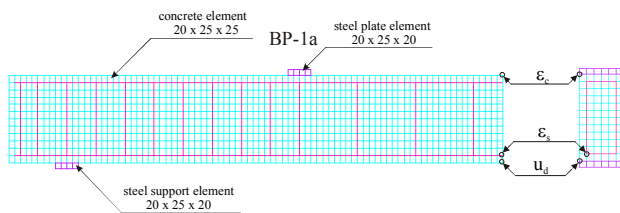


Fig. 2. FEM discretization of BP-1a beam with observation points of variations of deflection and strain

Rys. 2. Podział belki BP-1a na elementy skończone z oznaczonymi punktami obserwacji zmian przemieszczenia i odkształcenia

The results of the numerical calculations made by the Newton-Raphson method with adaptive descent and the definition of Crisfield's arc length were compared to the experimental data [1].

The Newton-Raphson method is an iterative process of solving nonlinear equations in the form of:

$$\left[K_i^T \right] \{ \Delta u_i \} = \{ F^a \} - \{ F_i^{nr} \} \quad (1)$$

$$\{ u_{i+1} \} = \{ u_i \} + \{ \Delta u_i \} \quad (2)$$

where: $\left[K_i^T \right]$ - tangent stiffness matrix, i - index corresponding to the current equilibrium iteration $\{ F_i^{nr} \}$ - vector of restoring loads representing the element internal loads.

The adaptive descent method presented in the work by Eggert et al. [2] is based on the change of solution path approximating the limit point and reversing along

the secant until obtaining the convergence of the numerical solution. In Newton-Raphson equation (1), the tangent stiffness matrix is described as a sum of two matrices:

$$\left[K_i^T \right] = \xi \left[K^S \right] + (1 - \xi) \left[K^T \right] \quad (3)$$

where: $\left[K^S \right]$ - secant stiffness matrix, $\left[K^T \right]$ - tangent stiffness matrix, ξ - adaptive descent parameter.

The method is based on setting adaptive descent parameter ξ during the equilibrium iterations. The secant stiffness matrix is generated while solving linear and non-linear tasks concerning plasticity, stress stiffness of the construction with large strain and crushing concrete with consideration for the post-cracking stress relaxation.

In the method of Crisfield's arc-length presented in Figure 3, equation (1) depends on load factor λ :

$$\left[K_i^T \right] \{ \Delta u_i \} = \lambda \{ F^a \} - \{ F_i^{nr} \} \quad (4)$$

In this method, changeable load factor λ is calculated in balance equations in the procedure of finite elements and has a value from the range $\langle -1, 1 \rangle$.

The equation has the incremental form at substep n and iteration i :

$$\left[K_i^T \right] \{ \Delta u_i \} - \Delta \lambda \{ F^a \} = (\lambda_0 + \Delta \lambda_i) \{ F^a \} - \{ F_i^{nr} \} \quad (5)$$

where $\Delta \lambda$ - incremental load factor.

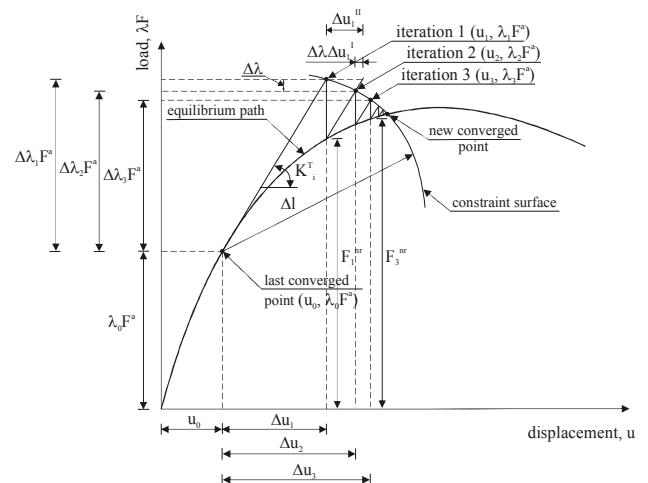


Fig. 3. Crisfield's arc-length method [3]

Rys. 3. Metoda długości łuku według Crisfielda [3]

Mather [4] proved that it should be theoretically possible to express the criteria of concrete crushing in all possible combinations of stresses with one parameter - the uniaxial compressive strength of concrete. Generally, with the value of concrete strength under compression, it is possible to define a complete set of material

profitable for construction safety. Applying too low strain values for the compression of high strength concrete in the model, in accordance with e.g. Model Code 90 [7], results in a significant decrease in the failure curves of the construction elements. The construction properties of the BP-1a beam are characterised by the following parameters of constituting models:

High strength concrete

- uniaxial compressive strength, experimentally defined by Kamińska [1], $f_c = 81.2$ MPa
- modulus of elasticity, calculated according to ACI 363 norm $E_c = 3.32\sqrt{f_c} + 6.9$, $E_c = 36817$ MPa
- uniaxial tension strength, calculated according to ACI 363 norm, $f_t = 0.54\sqrt{f_c}$, $f_t = 4.87$ MPa
- Poisson's ratio $\nu_c = 0.15$
- concrete density $\rho_c = 2600$ kg/m³
- compressive strain in concrete at peak stress f_c , $\epsilon_{c1} = 6\text{‰}$
- ultimate compressive strain in concrete $\epsilon_{cu} = 12\text{‰}$
- shear transfer coefficients for open crack $\beta_t = 0.5$, estimated on basis of author's numerical analyses
- shear transfer coefficients for closed crack $\beta_c = 0.99$

Reinforced steel

- modulus of elasticity for $\phi 6$ rods made of A-II steel, $\phi 10$ rods made of A-III steel $E_s = 200$ GPa
- yield stress for $\phi 10$ rods made of A-III steel $f_y = 410$ MPa, for $\phi 6$ rods made of A-II steel $f_y = 355$ MPa
- Poisson's ratio $\nu_s = 0.3$
- steel density $\rho_s = 7800$ kg/m³

Steel support and steel loading plate

- modulus of elasticity $E_s = 210$ GPa
- Poisson's ratio $\nu_s = 0.3$
- steel density $\rho_s = 7800$ kg/m³.

In the second version of the numerical solution, the concrete model is described by the five-parameter failure surface of high strength concrete which is compressed and tensed, in accordance with the William-Warnke theory (Fig. 6) and author's own proposal of the surface evolution in the function of its deformation (Fig. 5).

William and Warnke [5] presented a more detailed approximation of the concrete failure surface with a five-parameter model. In order to describe the parabolic shape of the failure surface meridians, the tree-parameter model was supplemented with two additional parameters. The criterion of concrete fracture in the complex stress condition is described by the equation:

$$\frac{F}{f_c} - S \geq 0 \tag{7}$$

where: F - the function of the principal stress state $\sigma_{xp}, \sigma_{yp}, \sigma_{zp}$ in the direction of the Cartesian coordinate system x, y, z , S - failure surface dependant on the principal stresses $\sigma_1, \sigma_2, \sigma_3$, where $\sigma_1 = \max(\sigma_{xp}, \sigma_{yp}, \sigma_{zp})$, $\sigma_3 = \min(\sigma_{xp}, \sigma_{yp}, \sigma_{zp})$ and $\sigma_1 \geq \sigma_2 \geq \sigma_3$ and five parameters: f_c - ultimate uniaxial compressive strength (causing crush), f_t - ultimate uniaxial tensile strength (causing failure), f_{cb} - ultimate biaxial compressive strength (causing crush), f_1 - ultimate compressive strength for a state of biaxial compression superimposed on hydrostatic stress state σ_h^a (causing crush) and f_2 - ultimate compressive strength for a state of uniaxial compression superimposed on hydrostatic stress state σ_h^a .

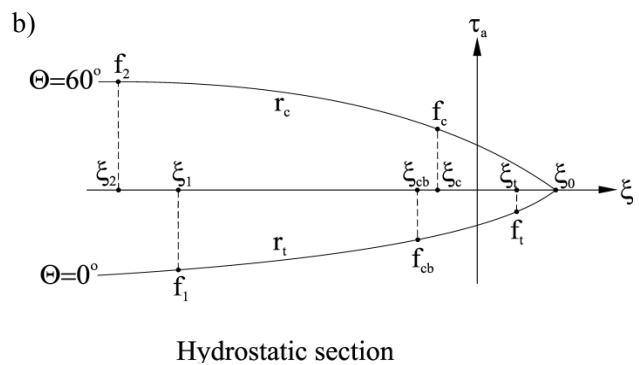
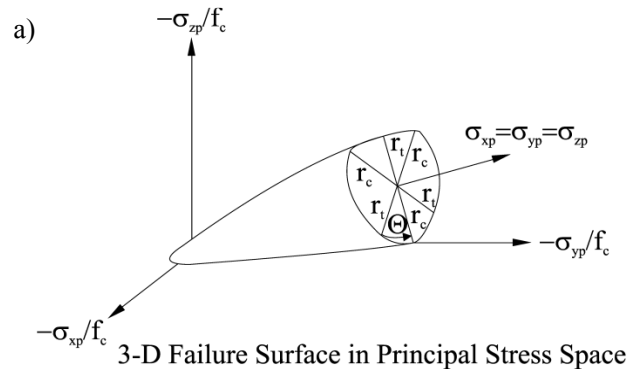


Fig. 6. Construction of five-parameter failure surface: in principal strain space (a) and in hydrostatic section (b)
 Rys. 6. Konstrukcja pięcioparametrowej powierzchni granicznej: w obszarze naprężeń głównych (a) i w przekroju hydrostatycznym (b)

The concrete failure surface is used as a criterion of destruction according to the following interpretation. The material is destroyed if inequality (7) is fulfilled. The state of failure can be distinguished as the state of cracking, if any principal stress is tensing, or in the state of crushing, if all the principal stresses are compressing.

The failure surface is defined by five strength parameters $f_c, f_t, f_{cb}, f_1, f_2$ and the state of hydrostatic

stress σ_h^a . The description of concrete failure is defined in four domains of stresses:

- $0 \geq \sigma_1 \geq \sigma_2 \geq \sigma_3$ (compression - compression - compression)
- $\sigma_1 \geq 0 \geq \sigma_2 \geq \sigma_3$ (tensile - compression - compression)
- $\sigma_1 \geq \sigma_2 \geq 0 \geq \sigma_3$ (tensile - tensile - compression)
- $\sigma_1 \geq \sigma_2 \geq \sigma_3 \geq 0$ (tensile - tensile - tensile).

In each range of strain, independent functions F_1, F_2, F_3, F_4 and S_1, S_2, S_3, S_4 describe the function state of stresses F and failure surface S .

The presented model illustrates the main features of concrete failure and determines the conical surface with the curvilinear slant height and the base constituted from three elliptic segments. The values of the parameters characterising this model are easy to determine with standard strength tests. It contains all three stress constants equal to average stress σ_h, F and angle θ . Moreover, it ensures smoothness of the failure surface in a wide range of parameters and describes four other models of failure surface that are used in the problems of concrete destruction in previously determined constant parameters.

Apart from the above presented parameters of constitutive models, the properties of the construction material of the BP-1a beam are defined by additional parameters describing the failure surface of high strength concrete, calculated with the equations presented in the works by William and Warnke [5]:

Additional parameters for high strength concrete

- ultimate biaxial compressive strength, $f_{cb} = 1.2f_c$, $f_{cb} = 97.4$ MPa
- ultimate compressive strength for state of biaxial compression superimposed on hydrostatic stress state σ_h^a , $f_1 = 1.45f_c$, $f_1 = 117.7$ MPa
- ultimate compressive strength for state of uniaxial compression superimposed on hydrostatic stress state σ_h^a , $f_2 = 1.725f_c$, $f_2 = 140.1$ MPa
- ambient hydrostatic stress state describing average distribution of normal stresses $\sigma_h = 1.73f_c$, $\sigma_h = 140.5$ MPa
- multiplier for amount of tensile stress relaxation $T_c = 1$.

The material models in the third version of the numerical solutions are identical to the above presented first proposal of the numerical solution. In the first two variants of the solution, Crisfield's arc-length method was used. Yet, in the third proposition the Newton-Raphson method with adaptive descent was used.

All the numerical calculations were made for an elastic and perfectly plastic model of reinforced steel (Fig. 7) and the elastic and brittle model of concrete, with softening in tension (Fig. 5b).

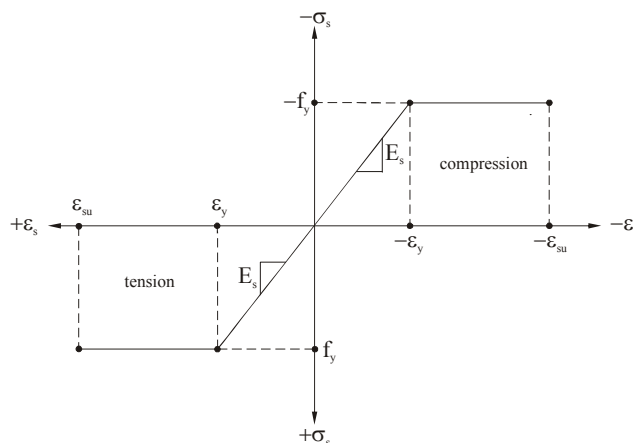


Fig. 7. Stress-strain curve for steel reinforcement used for analyses of reinforced concrete beam

Rys. 7. Zależność napężenie-odkształcenie dla stali zbrojeniowej zastosowana w analizach modelowej belki żelbetowej

ANALYSIS OF FAILURE CONDITION

Figure 8 presents the maps of crack patterns for various values of load obtained for three proposals of numerical solution for a model BP-1a beam. In the first and third numerical solution, the border surface of compressed and tensed high strength concrete is described by three material parameters, while in the second solution, the border surface is characterised by five parameters. In both solutions in Crisfield's method, the first cracks are formed in the section of constant moment for destructing load F_{cr} , therefore at the same moment as in the experimental value of the destructing load $F_{cr} = 15$ kN. The difference between the calculated and experimental value of the destructing load is c.a. 0.7%. Yet, in the Newton-Raphson method with adaptive descent the first crack is made in the section of typical bending for the load value $F_{cr} = 15.2$ kN, which makes c.a. a 2% difference in comparison to the numerical methods of arc-length.

In the first two numerical solutions, the flexural cracks propagate in the area of constant moment up to the load of 20 kN. Further increase causes propagation of the crack zone horizontally towards the support. In the third solution, the processes of cracking are quicker up to the moment of steel plastification. In all of the presented solutions, a significant increase in cracks can be observed for the load of 25 kN after reinforcing steel plastification. The cracks caused by compression in the load application zone and crushing in the bending zone are clearly noticeable. In both solutions with Crisfield's method, identical images of smeared cracks were obtained up to the load of 25 kN. In the final stages of loading, from the load of 27 kN up to the destruction moment, enhanced devastation was observed in the bending area that was characterised by new cracks in the surfaces perpendicular to the then non-cracked surfaces, accompanied by a relatively constant number of cracks in the supporting area.

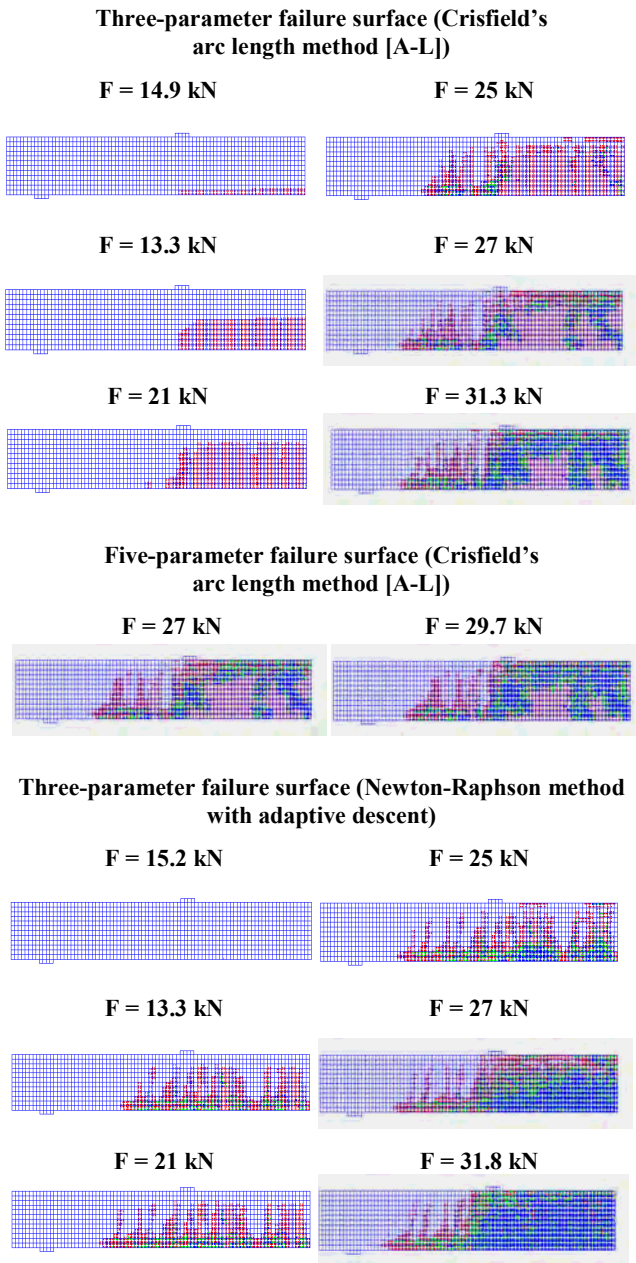


Fig. 8. Maps of smeared cracks for different levels of load values
Rys. 8. Mapy rys rozmytych dla różnych poziomów obciążenia

In the numerical solutions, the limit values of load were recorded for the following values $F_u = 31.3$ kN, $F_u = 29.7$ kN and $F_u = 31.8$ kN and were interpreted as the condition that is obtainable for such a value of load for which the increase in displacement at small values of load increase makes the numerical solutions not converge. Although in Kaminska's experiment [1] beam destruction was not observed, the value of maximum load calculated from the condition of deformation, $F_u = 30$ kN, approximates the value of destruction load calculated in the numerical solutions. In Figure 9, the image of real cracks in a full BP-1a beam is presented against the numerical images of smeared cracks for the left half of the beam, with the same value of load $F = 23$ kN.

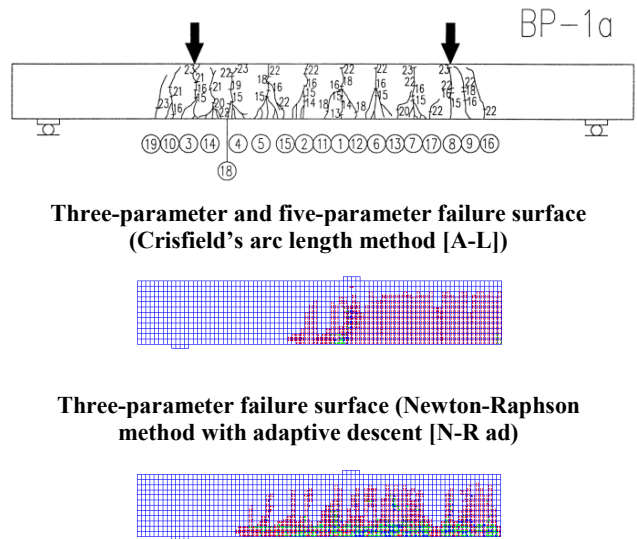


Fig. 9. Experimental [1] and numerical images of cracking BP-1a beam for load $F = 23$ kN
Rys. 9. Eksperymentalny [1] i numeryczne obrazy zarysowania belki BP-1a dla sily $F = 23$ kN

SUMMARY

The obtained numerical results supported by experimental results prove the fact that the fragility of high strength concretes in flexural beams is significantly limited by the good relation between the concrete and the reinforcement. The clear correlation of the experimental and numerical results depends on appropriate selection of the linear and nonlinear material properties.

All the obtained numerical results are in qualitative agreement with the experimental results in terms of their location, direction and concentration. In the case of the Newton-Raphson method with adaptive descent, a slightly larger zone of smeared cracks was observed. The numerical images of smeared cracks obtained by Crisfield's arc length method are best to reflect the real failure surfaces in terms of quantity. However, the images of cracks obtained by the Newton-Raphson method are characterised by better location and concentration. Even better images of cracks in the solutions obtained by Crisfield's method can be obtained by limiting the minimum step of load increase, which requires a longer time for numerical calculations.

REFERENCES

[1] Kamińska M.E., Doświadczalne badania żelbetowych elementów prętowych z betonu wysokiej wytrzymałości. KILiW, PAN, Łódź 1999.
[2] Eggert, G.M., Dawson, P.R., Mathur K.K., An adaptive descent method for nonlinear viscoplasticity, International Journal for Numerical Methods in Engineering 1991, 31, 1031-1054.
[3] Crisfield M.A., An arc-length method including line searches and accelerations, International Journal for Numerical Methods in Engineering 1983, 19, 1269-1289.

- [4] Mather B., What do we need to know about the response of plain concrete and its matrix to combined loadings? Proceedings 1st Conference on the Behavior of Structural Concrete Subjected to Combined Loadings, West Virginia University 1969, 7-9.
- [5] Willam K.J., Warnke E.P., Constitutive Model for the Triaxial Behavior of Concrete. Proceedings, International Association for Bridge and Structural Engineering, ISMES, Bergamo, Italy 1975, 19.
- [6] Smarzewski P., Stolarski A., Modelowanie zachowania niesprężystej belki żelbetowej, Biuletyn WAT 2007, LVI, 2, 147-166.
- [7] Comité Euro-Internacional du Béton: High Performance Concrete. Recommended to the Model Code 90. Research Need, Bulletin d'Information 1995, 228.